Physica A 389 (2010) 5022–5027

Contents lists available at ScienceDirect

Physica A

journal homepage: www.elsevier.com/locate/physa

Entropy analysis of the dynamics of El Niño/Southern Oscillation during the Holocene

Patricia M. Saco [a,b], Laura C. Carpi [a,c], Alejandra Figliola [d], Eduardo Serrano [e], Osvaldo A. Rosso [c,f,*]

[a] Civil, Surveying and Environmental Engineering, The University of Newcastle, University Drive, Callaghan NSW 2308, Australia

[b] Departamento de Hidráulica, Facultad de Ciencias Exactas, Ingeniería y Agrimensura, Universidad Nacional de Rosario, Avenida Pellegrini 250, 2000 Rosario, Argentina

[c] Departamento de Física, Instituto de Ciências Exatas, Universidade Federal de Minas Gerais, Av. Antônio Carlos, 6627 - Campus Pampulha, 31270-901 Belo Horizonte - MG, Brazil

[d] Instituto del Desarrollo Humano, Universidad Nacional de General Sarmiento, Juan María Gutiérrez 1150, Los Polvorines, Buenos Aires, Argentina

[e] Centro de Matemática Aplicada, ECyT, Universidad Nacional de San Martín, Irigoyen 3100, San Martín, Buenos Aires, Argentina

[f] Chaos & Biology Group, Instituto de Cálculo, Facultad de Ciencias Exactas y Naturales, Universidad de Buenos Aires, Pabellón II, Ciudad Universitaria, 1428 Ciudad Autónoma de Buenos Aires, Argentina

ARTICLE INFO

Article history:
Received 30 April 2010
Received in revised form 18 June 2010
Available online 13 July 2010

Keywords:
Entropy
Time series analysis
Probability distribution
ENSO dynamics

ABSTRACT

This study explores temporal changes in the dynamics of the Holocene ENSO proxy record of the Laguna Pallcacocha sedimentary data using two entropy quantifiers. In particular, we analyze the possible connections between changes in entropy and epochs of rapid climate change (RCC). Our results indicate that the dynamics of the ENSO proxy record during the RCC interval 9000–8000 BP displays very low entropy (high predictability) that is remarkably different from that of the other RCCs of the Holocene. Both entropy quantifiers point out to the existence of cycles with a period close to 2000 years during the mid-to-late Holocene. Within these cycles, we find a tendency for entropy to increase (predictability to decrease) during the two longer RCC periods (6000–5000 and 3500–2500 BP) which might be associated with the reported increased aridity of the low tropics.

1. Introduction

El Niño/Southern Oscillation (ENSO), an occasional shift in winds and ocean currents centered in the South Pacific region, is linked to anomalous global climate patterns responsible for producing worldwide socio-economical impacts. Interest on the future behaviour of ENSO under the influence of enhanced greenhouse gases has led to renewed research into its long term history. Though several proxy records of ENSO have become recently available [1, and the references therein] the understanding of its complex dynamics over millennial time scales is still limited.

In this work we study the dynamics of the Holocene proxy ENSO record corresponding to the Laguna Pallcacocha sedimentary data [2,3]. Specifically, we analyze temporal changes in dynamics over the last 11 000 years using entropy quantifiers. The proxy record (Fig. 1) was obtained from the analysis of clastic laminae deposition in two 8 m sediment cores retrieved from the Pallcacocha Lake in Ecuador. Moy and coworkers [2] explain that during warm ENSO events,

* Corresponding author at: Departamento de Física, Instituto de Ciências Exatas, Universidade Federal de Minas Gerais, Av. Antônio Carlos, 6627 - Campus Pampulha, 31270-901 Belo Horizonte - MG, Brazil.

E-mail addresses: Patricia.Saco@newcastle.edu.au (P.M. Saco), lauracarpi@gmail.com (L.C. Carpi), alejandra.figliola@gmail.com (A. Figliola), eduardo.eduser@gmail.com (E. Serrano), oarosso@fibertel.com.ar, oarosso@gmail.com (O.A. Rosso).

0378-4371/$ – see front matter © 2010 Elsevier B.V. All rights reserved.
doi:10.1016/j.physa.2010.07.006

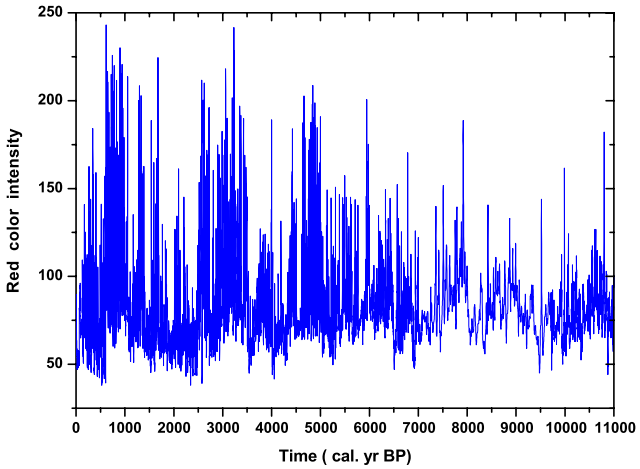

Fig. 1. ENSO proxy data from the Laguna Pallcacocha in Ecuador [2,3].

convective precipitation triggers erosion and debris-flow activity, increasing the sediment load contributed to the lake. They assumed that the light-colored, inorganic clastic sediment laminae in the sediment core were deposited during ENSO-driven episodes. This hypothesis was based on the observation that light-colored laminae deposited in the more recent 200 years generally correlated with known moderate to severe El Niño events from instrumental and historical records. To quantify the distribution of the light-colored laminae in the lake sediments, the surface of the core sections was digitally scanned and the red color intensity was used to generate the record of ENSO variability. Then, an age model based on radiocarbon chronology was used to create the time series of red color intensity for the Holocene.

As is explained by Moy et al. [2,3], the age model for the new record is based on the same radiocarbon chronology used by Rodbell et al. [4]. The laminae dated by AMS ^{14}C of terrestrial microfossils in Ref. [4] record are distinctive and could be confidently identified in the new cores. By creating a composite section from overlapping drives, Moy et al. were able to improve on the original age model. They adopted the constant carbon accumulation model and an event model to allocate time between dated intervals [4,5]. The constant carbon accumulation model assumes that the rate of organic carbon deposition has remained nearly constant between radiocarbon-dated intervals through the Holocene, and this continuous sedimentation was punctuated by nearly instantaneous clastic depositional events.

The original Pallcacocha Lake data [3] has been interpolated to a sample time of one year using a cubic Hermite polynomial. The corresponding time series of $M = 11\,000$ data has been considered in the analysis and is displayed in Fig. 1 ($T_{\text{sample}} = 1$ year). Using wavelet analysis on this proxy record, Moy et al. [2] found a millennial-scale oscillation coherent throughout the Holocene but displaying less significant variance in the early Holocene. They identified a shift in variance around 5000 BP, from a 1500 yr period in the middle/early Holocene to a 2000 yr period in the late Holocene. Wang and Tsonis [6] found that this proxy exhibits long-range correlations extending to timescales of half a millennium which explains the presence of long lasting extreme (El Niño or La Niña) events. Tsonis [7] analyzed the record using several nonlinear dynamic techniques and concluded that the shift in behaviour around 5000 BP could be explained as a bifurcation in the dynamics given by a transition from chaotic to hyper-chaotic dynamics. In our work using entropy quantifiers, we also find evidence of a shift in dynamics and cyclic behaviour. In addition, we have been able to localize these cycles in time and to analyze connections between changes in entropy and epochs of rapid climate change (RCC) during the Holocene [1, 8].

2. Methodology: the Shannon entropy measure and its evaluation

One approach to exploring changes in the dynamics of the proxy ENSO time series is through the use of entropy quantifiers originally derived in Information Theory. Information Theory was initially developed to deal with compression and communication of data and has significantly contributed to fields such as statistical mechanics, computer science, statistical inference, and nonlinear dynamics. It has also been used to analyze changes in the dynamics of natural processes in neurosciences, ecology, economics and various fields of geosciences. A key quantifier in this theory is entropy, the fundamental basis of the second law of thermodynamics and a measure of the randomness, uncertainty or disorder of a physical process. For a given time series $X = \{x_t, t = 1, \ldots, M\}$ of length M, the Shannon entropy [9] is defined as:

$$S[P] = -\sum_{j=1}^{N} p_j \cdot \ln p_j \tag{1}$$

where $P = \{p_j : j = 1, \ldots, N\}$ the probability distribution function (PDF) describing the empirical distribution of X, and N is the number of possible states. If $S[P] = 0$ we are in a position to predict with certainty *which* of the possible

outcomes j whose probabilities are given by the p_j will actually take place. Our knowledge of the underlying process described by the probability distribution is, in this instance, maximal. On the other hand, our ignorance is maximal for a uniform distribution, $P_e = \{1/N, \ldots, 1/N\}$, and in this case $S[P_e] = S_{max} = \ln(N)$. The "normalized Shannon entropy" is defined as $H[P] = S[P]/S_{max}$.

A key point for the estimation of $S[P]$ is the identification of the probability distribution function, P, that more adequately describes the dynamical properties of the system or time series under study. Many procedures have been proposed for a proper selection of P, for instance techniques based on amplitude statistics (histograms), symbolic dynamics, Fourier analysis, and wavelet transforms [10–12, and the references therein]. The various approaches are all able to capture the global aspects of the dynamics, but they are not equivalent in their ability to discern physical details [10].

In this work we use two different approaches to capture different aspects of the dynamics. The first approach is broadly used, and computes the PDF (P) using a histogram of amplitudes. In this case, the empirical PDF is obtained by classifying each value in the time series (x_t) into a number of equally spaced and non-overlapping bins. Hereafter, we will denote the normalized Shannon entropy obtained using amplitude histograms as $H^{(Hist)}$. A drawback of this approach is that it does not account for the temporal organization (or "causality") of consecutive values in the time series.

The second approach that we use corresponds to that introduced by Bandt and Pompe and evaluates the PDF associated with a time series data using a symbolization technique [13,14]. The symbolic data is created by ranking and reordering the values of the (embedded) time series (see methodology below). *Causal information* is, consequently, incorporated into the construction process that yields P and leads to noticeable improvements in the performance of information quantifiers [12,15]. Hereafter, we will refer to the normalized Shannon entropy estimated using the Bandt & Pompe approach simply as permutation entropy and denoted by $H^{(BP)}$.

The procedure for the determination of P using the Bandt & Pompe approach involves the following steps [13,14]: (a) For the time series $X = \{x_t : t = 1, \ldots, M\}$ we choose an embedding dimension $D > 1$. (b) We assign to each "time s" a D-dimensional vector of values corresponding to times $s, s-1, \ldots, s-(D-1)$ generated by

$$(s) \mapsto (x_{s-(D-1)}, x_{s-(D-2)}, \ldots, x_{s-1}, x_s). \tag{2}$$

Clearly, the greater the value of D, the more information on "the past" that is incorporated into these vectors. (c) Each vector classified into one of D! possible ordinal patterns given by the permutation $\pi = (r_0, r_1, \ldots, r_{D-1})$ of $(0, 1, \ldots, D-1)$ defined by

$$x_{s-r_{D-1}} \leq x_{s-r_{D-2}} \leq \cdots \leq x_{s-r_1} \leq x_{s-r_0}. \tag{3}$$

In order to get a unique result we consider that $r_i < r_{i-1}$ if $x_{s-r_i} = x_{s-r_{i-1}}$. Thus, for all the $D!$ possible permutations π of order D, the probability distribution $P = \{p(\pi)\}$ is defined by

$$p(\pi) = \frac{\sharp\{s | s \leq M - D + 1;\ (s) \text{ has type } \pi\}}{M - D + 1} \tag{4}$$

where the symbol $\sharp$ stands for "number".

The advantages of the Bandt & Pompe method are (i) simplicity, (ii) fast calculation process, (iii) robustness in the presence of noise, and (iv) invariance with respect to nonlinear monotonous transformations. The Bandt & Pompe methodology is not restricted to time series representative of low dimensional dynamical systems but can be applied to any type of observational time series (regular, chaotic, noisy), with a very weak stationary assumption (for $k = D$, the probability for $x_t < x_{t+k}$ should not depend on t).

The embedding dimension D plays an important role in the construction of the probability distribution because it determines the number of accessible states $D!$. Also, it conditions the minimum acceptable length $M \gg D!$ of the time series needed to obtain reliable statistics. Bandt and Pompe suggest, for practical purposes, to work with $3 \leq D \leq 7$.

To facilitate the discussion in the following section, we give a short interpretation of the permutation entropy quantifier. The Bandt & Pompe PDF is estimated by classifying sequences of D data points (in our case annual events) according to the order of their temporal relative magnitudes. Let us assume in the following that $D = 5$ and $M = 1000$. For example, if the relative magnitude of the events is as follows: *highest, lowest, third lowest, fourth lowest, second lowest,* then this sequence will be classified into a pattern by ranking and reordering the sequence as follows: event 2 $\leq$ event 5 $\leq$ event 3 $\leq$ event 4 $\leq$ event 1, and labeled "ordinal pattern 25341". There are $D!$ possible ordinal patterns, corresponding to the possible permutations of relative magnitude of sequences of D events. To obtain the empirical Bandt & Pompe distribution, the 996 successive sequences of five data points in the 1000 data series are classified into the possible $D!$ ordinal patterns (in our case $D! = 120$). $H^{(BP)} = 1$ (highest value) means that the relative magnitude of sequences of five ordered events is unpredictable (all patterns are equally possible) while a low value means that they are more predictable as some patterns appear more frequently than others. Recent research has shown that some of the possible $D!$ ordinal patterns might be missing in an observational time series. Missing order patterns have been shown to appear in chaotic time series and in random time series with long term correlations (persistence) [16,17]. A large number of missing patterns means that ordinal patterns are more predictable and will result in a low permutation entropy.

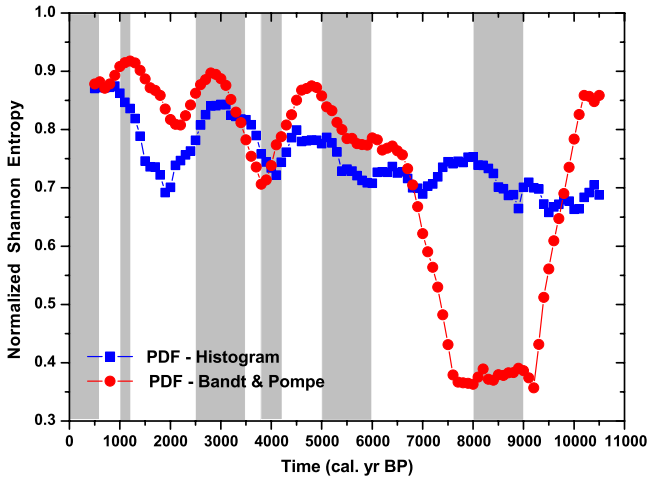

Fig. 2. Entropy quantifiers for the ENSO proxy time series using a sliding time window of 1000 data values and a lag of 100 data values between successive windows. To compute the amplitude histogram we consider $N_{\text{bin}} = 100$ in the interval [38.06, 243.06]. The Bandt and Pompe PDF was estimated using ordinal patterns of length of $D = 5$. The grey bands correspond to the major periods of Holocene rapid climate change (RCC).

3. Results

The evolution of the normalized Shannon entropy corresponding to the proxy ENSO data (Fig. 1) was evaluated using both amplitude histograms and the Bandt & Pompe methodology to obtain the two entropy quantifiers ($H^{(\text{Hist})}$ and $H^{(\text{BP})}$) described in the previous section. We computed the evolution of the quantifiers through time using a sliding time window of 1000 data (1000 years) values with a lag of 100 data (100 years) values between successive windows. A sliding window was used to allow for a better localization of changes in the dynamics of ENSO through time. The amplitude histogram was evaluated using $N_{\text{bins}} = 100$ in the interval [38.06, 243.06] (defined by the minimum and maximum amplitude values of the complete time series).

ENSO is a climate pattern that occurs across the tropical pacific ocean on average every five years, but over a period which varies from three to seven years. Then for the estimation of the Bandt & Pompe PDF, we used a length of patterns (embedding dimension) of $D = 5$. This is the same value used by Tsonis et al. for the embedding dimension in the characterization of this ENSO proxy time series using nonlinear dynamics metrics tools [6,7].

The pattern and window lengths were selected to obtain a good temporal localization of changes in the dynamics (up to a millennial time scales) without compromising the data needs to obtain reliable statistics for the permutation entropy quantifier. We should point out that the results obtained when we considered $D = 4$ and $D = 6$, were similar to those shown below, however, in the last case, it was necessary to increase the window length in order to satisfy the condition $M \gg D!$.

The main difference between both entropy measures is that, unlike $H^{(\text{Hist})}$, $H^{(\text{BP})}$ is invariant with respect to strictly monotonous distortions of the data. We should point out that the present proxy data is based on "red color intensity" of sedimentary data and related to rainfall by a function which is unknown but very likely to be nonlinear. However, due to its invariance, $H^{(\text{BP})}$ applied to any other data series that is strictly monotonously related to "red color intensity" would yield the same results. Therefore, in general, ordinal data processing tools based on ranked numbers would lead to results that are more robust (and useful) for proxy data analysis than those obtained using tools based on metric properties.

Fig. 2 displays the results of both entropy quantifiers. We also show in this figure, as grey bands, the major periods of Holocene rapid climate change (RCC) defined by Denton and Karlén [8] from glacier fluctuation records (tuned to high-resolution GISP2 record). RCC periods were identified by Denton and Karlén [8] at 9000–8000 BP, 6000–5000 BP, 4200–3800 BP, 3500–2500 BP, 1200–1000 BP, and since 600 BP. These periods have been frequently used as a framework for the examination of Holocene climate variability [1, and the references therein].

3.1. Amplitude histogram entropy quantifier

Fig. 2 shows an overall increasing trend for $H^{(\text{Hist})}$ from 11 000 BP to present, that can be interpreted as an increase in uncertainty. This result is in agreement with previous results from Tsonis [7] who found a decrease in predictability between the first (11 000–5000 BP) and second period (5000 BP–present). However, the results from Fig. 2 also show that the increase in $H^{(\text{Hist})}$ (or decrease in predictability) is not gradual throughout the period and there are substantial fluctuations or cycles with shorter periods of increasing and decreasing entropy. These cycles have an approximate period of 2000 years (9000 to 7000 BP, 6000 to 4000 BP, 4000 to 2000 BP). Within cycles of $H^{(\text{Hist})}$, there is a tendency for local entropy maxima (or minimum predictability) to coincide with periods of rapid climate change (RCC). Both the local maxima and the amplitude

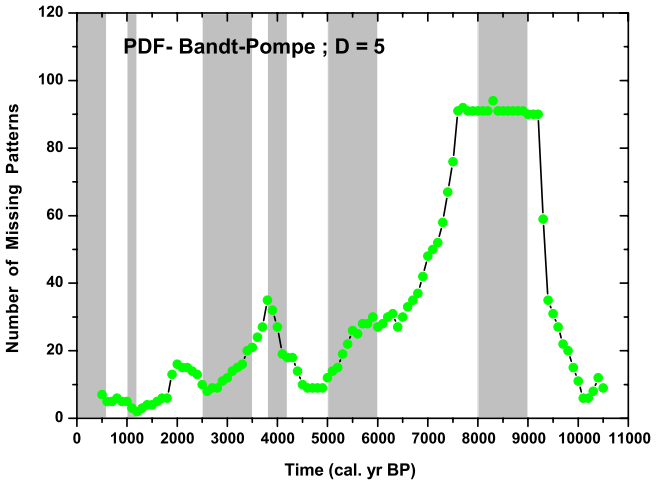

Fig. 3. Missing ordinal patterns obtained for the ENSO proxy obtained using a sliding time window of 1000 data values, a lag of 100 values between successive windows, and $D = 5$. The grey bands correspond to the major periods of Holocene rapid climate change (RCC).

of the "cycles" in $H^{(\mathrm{Hist})}$ also show an increasing trend towards the present. An interesting observation is that most RCC periods seem to be associated with high rates of entropy ($H^{(\mathrm{Hist})}$) gain, suggesting that variability and uncertainty of ENSO increased during these RCCs.

3.2. Permutation entropy quantifier

As seen in Fig. 2, $H^{(\mathrm{BP})}$ points out a quite different ENSO dynamics between the early (11 000–6500 BP) and middle-to-late Holocene (6500 BP to present) that is not captured by the $H^{(\mathrm{Hist})}$ quantifier. The period 11 000–6500 BP presents the lowest variability, see Fig. 1, as well as an obvious trend around 9500–8800 BP (upward) and 8800–8000 BP (downward). As mentioned before, the Bandt & Pompe methodology is based on ordinal data analysis, and unlike $H^{(\mathrm{Hist})}$, displays robustness against trends present in the data.

The initial values of $H^{(\mathrm{BP})}$ at the early Holocene are quite high ($H^{(\mathrm{BP})} = 0.85$). These values indicate that the ordinal patterns (describing the relative magnitude of five successive events) are quite unpredictable. Soon after 10 000 BP, a rapid decrease in permutation entropy occurs over a period of less than 1000 years reaching a minimum $H^{(\mathrm{BP})}$ at around 9200 BP. This is followed by an interval of remarkable quasi-steady entropy occurring over more than 1500 years, with a significantly low $H^{(\mathrm{BP})}$ (close to 0.37). The dramatic decrease in the $H^{(\mathrm{BP})}$ quantifier suggests a remarkable shift in dynamics towards a more organized or predictable condition which lasts for more than a millennia. Further inspection of the Bandt and Pompe ordinal patterns, show the existence of numerous missing ordinal patterns during this period (Fig. 3). As explained in the previous section, missing ordinal patterns could be the result of either chaotic dynamics or random behaviour with long term correlations [17]. We should note that centered within this interval of quasi-steady low $H^{(\mathrm{BP})}$ with numerous missing ordinal patterns, is the 9000–8000 BP RCC period. Therefore, our results suggest that during this RCC period, the ENSO record has a dynamic behaviour that is distinctively different from that of the other RCCs of the Holocene. Following the end of this first Holocene RCC period, at around 7500 BP, there is another important change in dynamics that results in an abrupt increase in $H^{(\mathrm{BP})}$ (during a 1000 year period) to a value slightly higher than 0.75 at 6500 BP.

As opposed to the early Holocene, during the period starting in 6500 BP the permutation entropy quantifier, $H^{(\mathrm{BP})}$, follows a cyclic behaviour similar to that of $H^{(\mathrm{Hist})}$. During the mid-to-late Holocene period, $H^{(\mathrm{BP})}$ displays its highest regularity and predictability at 4000 BP (RCC).

4. Discussion and conclusions

As shown in the previous section, the two entropy quantifiers point out different aspects of the dynamics of the ENSO proxy during the Holocene. Our results indicate that the dynamics of the ENSO record during the RCC interval 9000–8000 BP is remarkably different from that of the other RCCs of the Holocene. As explained by Mayewski et al. [1], this RCC interval is the only one that coincides with a significant increase in volcanic aerosol production, and it occurred when bipolar ice sheet dynamics still had the potential for substantial effects on global climate. Both entropy quantifiers are low during this period and the number of missing patterns is very high suggesting higher predictability of ENSO.

Both entropy quantifiers point out to the existence of cycles (intervals of increasing and decreasing entropy) with a period close to 2000 years during the mid-to-late Holocene (approximately 6000 to 4000 BP, 4000 to 2000 BP). This cyclic dynamics is consistent with that observed by Moy et al. [2] using wavelet analysis. An interesting observation, that was not evident in previous work, is that within these two cycles there is a tendency for entropy to increase during the two longer RCC periods

of the mid-to-late Holocene (6000–5000 and 3500–2500 BP). This indicates that both amplitude variability, measured by $H^{(\mathrm{Hist})}$, and pattern variability, measured by $H^{(\mathrm{BP})}$, of the ENSO proxy tend to increase (predictability decreases) during these two longer RCCs. Interestingly, Mayewski and coworkers [1] noted that the longer RCCs coincide with maxima in the $\Delta^{14}C$ and ^{10}Be events suggesting a decline in solar output at these times. As opposed to the longer RCCs, Mayewski et al. [1] could not relate the minor RCC events (4200–3800 and 1200–1000 BP) to specific forcing mechanisms. This indicates that the solar decline during the major RCCs might be responsible for the increased entropy (decreased predictability) in the ENSO record, probably through the increased aridity and associated higher rainfall variability reported in the low tropics during these periods.

Acknowledgements

We wish to thank Dr. Martín Gómez Ravetti, and Dr. José Rodriguez for very useful discussions and comments on the current manuscript. This research has been partially supported by a scholarship from The University of Newcastle awarded to L.C. Carpi. A. Figliola and O.A. Rosso acknowledges partial support from the Consejo Nacional de Investigaciones Científicas y Técnicas (CONICET), Argentina. O.A. Rosso gratefully acknowledges support from CAPES, PVE fellowship, Brazil.

References

[1] P.A. Mayewski, E.E. Rohling, J.C. Stager, W. Karlén, K.A. Maasch, L.D. Meeker, E.A. Meyerson, F. Gasse, S. van Kreveld, K. Holmgren, J. Lee-Thorp, G. Rosqvist, F. Rack, M. Staubwasser, R.R. Schneider, E.J. Steig, Holocene climate variability, Quat. Res. 62 (2004) 243–255.
[2] C.M. Moy, G.O. Seltzer, D.T. Rodbell, D.M. Anderson, Variability of El Niño southern oscillation activity at millennial timescales during the holocene epoch, Nature 420 (2002) 162–165.
[3] C.M. Moy, G.O. Seltzer, D.T. Rodbell, D.M. Anderson, Laguna pallcacocha sediment color intensity data, IGBP PAGES/World Data Center for Paleoclimatology Data Contribution Series 2002–76, NOAA/NCDC Paleoclimatology Program, Boulder CO, 2002. Data available online at: http://www.ngdc.noaa.gov/paleo/pubs/moy2002.
[4] D.T. Rodbell, G.O. Seltzer, D.M. Anderson, M.B. Abbott, D.B. Enfield, J.H. Newman, An ∼15 000-year record of El Niño-driven alluviation in southwestern ecuador, Science 283 (1999) 516–520.
[5] C.M. Moy, A continuous record of late-quaternary El Nino-southern oscillation from the southern ecuadorian Andes, M.S. Thesis, Syracuse University, 2000.
[6] G. Wang, A.A. Tsonis, On the variability of ENSO at millennial timescales, Geophys. Res. Lett. 35 (2008) L17702.
[7] A.A. Tsonis, Dynamical changes in the ENSO system in the last 11,000 years, Clim. Dyn. 33 (2008) 1069–1074.
[8] G.H. Denton, W. Karlén, Holocene climatic variations: their pattern and possible cause, Quat. Res. 3 (1973) 155–205.
[9] C. Shannon, W. Weaver, The Mathematical Theory of Communication, University of Illinois Press, Champaign, IL, 1949.
[10] A.M. Kowalski, M.T. Martín, A. Plastino, O.A. Rosso, Bandt–Pompe–Tsallis quantifier and quantum-classical transition, Physica A 288 (2009) 4061–4067.
[11] L. De Micco, C.M. Gonzalez, H.A. Larrondo, M.T. Martín, A. Plastino, O.A. Rosso, Randomizing nonlinear maps via symbolic dynamics, Physica A 387 (2008) 3373–3383.
[12] O.A. Rosso, L. De Micco, H.A. Larrondo, M.T. Martín, A. Plastino, Generalized statistical complexity measure, Internat. J. Bifur. Chaos 20 (2010) 775–785.
[13] C. Bandt, B. Pompe, Permutation entropy: a natural complexity measure for time series, Phys. Rev. Lett. 88 (2002) 174102.
[14] K. Keller, M. Sinn, Ordinal analysis of time series, Physica A 356 (2005) 114–120.
[15] O.A. Rosso, H.A Larrondo, M.T. Martín, A. Plastino, M.A. Fuentes, Distinguishing noise from chaos, Phys. Rev. Lett. 99 (2007) 154102.
[16] J.M. Amigó, S. Zambrano, M.A.F. Sanjuán, True and false forbidden patterns in deterministic and random dynamics, Europhys. Lett. 79 (2007) 50001.
[17] L.C. Carpi, P.M. Saco, O.A. Rosso, Missing ordinal patterns in correlated noises, Physica A 389 (2010) 2020–2029.